

# Lateral integration of MEMS VCSEL and slow light amplifier boosting single mode power

Masanori Nakahama<sup>a)</sup>, Toshikazu Shimada, and Fumio Koyama

*Precision and Intelligence Laboratory, Tokyo Institute of Technology*

*R2-39, 4259 Nagatsuta, Midori-ku, Yokohama, 226–8503, Japan*

*a) masanori.nakahama@ms.pi.titech.ac.jp*

**Abstract:** We propose the lateral integration scheme of an MEMS tunable VCSEL and a slow light amplifier for increasing single-mode power. The modeling result predicts the maximum output power over several tens mW for a compact slow light amplifier monolithically integrated with an MEMS VCSEL. In addition, the efficient excitation of slow light in the integrated slow light amplifier is shown. A high coupling efficiency and a radiation angle from the amplifier are almost constant during wide wavelength tuning.

**Keywords:** tunable VCSEL, MEMS, semiconductor optical amplifier

**Classification:** Optoelectronics, Lasers and quantum electronics, Ultrafast optics, Silicon photonics, Planar lightwave circuits

## References

- [1] N. Yokouchi, T. Miyamoto, T. Uchida, Y. Inaba, F. Koyama, and K. Iga, “40 Å continuous tuning of a GaInAsP/InP vertical-cavity surface-emitting laser using an external mirror,” *IEEE Photonics Technol. Lett.*, vol. 4, no. 3, pp. 701–703, July 1992.
- [2] M. S. Wu, E. C. Vail, G. S. Li, W. Yuen, and C. J. Chang-Hasnain, “Tunable micromachined vertical cavity surface emitting laser,” *Electron. Lett.*, vol. 31, no. 19, pp. 1671–1672, Sept. 1995.
- [3] M. C. Larson and J. S. Harris, Jr., “Wide and continuous wavelength tuning in a vertical-cavity surface-emitting laser using a micromachined deformable-membrane mirror,” *Appl. Phys. Lett.*, vol. 68, no. 7, pp. 891–893, Feb. 1996.
- [4] C. J. Chang-Hasnain, “Tunable VCSEL,” *IEEE J. Sel. Topics Quantum Electron.*, vol. 6, no. 6, pp. 978–987, Nov. 2000.
- [5] J. Boucart, R. Pathak, D. Zhang, M. Beaudoin, P. Kner, D. Sun, R. J. Stone, R. F. Nabiev, and W. Yuen, “Long wavelength MEMS tunable VCSEL with InP-InAlGaAs bottom DBR,” *IEEE Photonics Technol. Lett.*, vol. 15, no. 9, pp. 1186–1188, Sept. 2003.
- [6] F. Riemenschneider, M. Maute, H. Halbritter, G. Boehm, M.-C. Amann, and P. Meissner, “Continuously tunable long-wavelength MEMS-VCSEL with over 40-nm tuning range,” *IEEE Photonics Technol. Lett.*, vol. 16, no. 10, pp. 2212–2214, Oct. 2004.
- [7] C. K. Kim, M. L. Lee, and C. H. Jun, “Electrothermally actuated Fabry-

- Perot tunable filter with a high tuning efficiency,” *IEEE Photonics Technol. Lett.*, vol. 16, no. 8, pp. 1894–1896, Aug. 2004.
- [8] M. C. Y. Huang, Y. Zhou, and C. J. Chang-Hasnain, “Nano electro-mechanical optoelectronics tunable VCSEL,” *Opt. Express*, vol. 15, no. 3, pp. 1222–1227, Feb. 2007.
- [9] H. Sano, A. Matsutani, and F. Koyama, “Athermal 850 nm Vertical Cavity surface emitting lasers with thermally actuated cantilever structure,” *Appl. Phys. Express*, vol. 2, 072101, June 2009.
- [10] H. Sano and F. Koyama, “Proposal of gain-matched VCSELs with a thermally actuated MEMS structure for wide temperature operations,” *IEICE Electron. Express*, vol. 6, no. 20, pp. 883–888, June 2009.
- [11] M. Nakahama, H. Sano, N. Nakata, A. Matsutani, and F. Koyama, “Giant wavelength-temperature dependence of MEMS VCSELs,” *CLEO2011*, CMI7, May 2011.
- [12] D. Huang, E. A. Swanson, C. P. Lin, J. S. Schuman, W. G. Stinson, W. Chang, M. R. Hee, T. Flotte, K. Gregory, C. A. Puliafito, and J. G. Fujimoto, “Optical coherence tomography,” *Science*, vol. 254, no. 5035, pp. 1178–1181, 1991.
- [13] V. J. Srinivasan, R. Huber, I. Gorczynska, J. G. Fujimoto, J. Y. Jiang, P. Reisen, and A. E. Cable, “High-speed, high-resolution optical coherence tomography retinal imaging with a frequency-swept laser at 850 nm,” *Opt. Lett.*, vol. 32, no. 4, pp. 361–363, 2007.
- [14] V. Jayaraman, J. Jiang, H. Li, P. Heim, G. Cole, B. Potsaid, J. G. Fujimoto, and A. Cable, “OCT Imaging up to 760 kHz Axial Scan Rate Using Single-Mode 1310 nm MEMs-Tunable VCSELs,” *CLEO:2011 - Laser Applications to Photonic Applications*, OSA Technical Digest (CD) (Optical Society of America, 2011), paper PDPB2.
- [15] T. Shimada and F. Koyama, “Lateral integration of VCSEL with slow light amplifier/modulator,” *IEEE Photonics Society 23rd Annual Meeting, IEEE2010*, TuQ4, Nov. 2010.
- [16] Y. Sakurai and F. Koyama, “Control of Group Delay and Chromatic Dispersion in Tunable Hollow Waveguide with Highly Reflective Mirrors,” *Jpn. J. Appl. Phys.*, vol. 43, no. 8B, pp. 5828–5831, Aug. 2004.
- [17] A. S. Sudbo, “Film mode matching: a versatile numerical method for vector mode field calculations in dielectric waveguides,” *Pure Appl. Opt.*, vol. 2, pp. 211–233, 1993.
- [18] X. Gu, T. Shimada, A. Fuchida, A. Matsutani, A. Imamura, and F. Koyama, “Beam steering in GaInAs/GaAs slow-light Bragg reflector waveguide amplifier,” *Appl. Phys. Lett.*, vol. 99, pp. 211107-1–211107-3, 2011.

## 1 Introduction

Vertical cavity surface emitting lasers (VCSELs) with micro electro mechanical system (MEMS) have been attracting much interest as either a widely tunable light source or an athermal semiconductor laser [1, 2, 3, 4, 5, 6, 7, 8, 9, 10, 11]. A widely tunable MEMS VCSEL is a good candidate for use in optical coherence tomography (OCT) [12]. Since a VCSEL has a very short cavity, a slight change in a cavity length enables continuous and wide wavelength tuning. Recently, high-speed OCT imaging was demonstrated

by using a widely tunable 1300 nm-band MEMS VCSEL [13]. However, the single-mode power of a tunable MEMS VCSEL has been limited below a few mW, which needs an external optical amplifier boosting the output power for use in OCT applications [13]. The drawback of low output power in MEMS tunable VCSELs has limited their available applications either in optical communications or in optical sensing. A challenge is to realize high power single-mode operation with wide tunability. We proposed and demonstrated the lateral integration of a VCSEL and slow light amplifier [14]. In this paper, we present the modeling of the lateral integration of a tunable MEMS VCSEL and slow light amplifier to boost a single-mode power. The maximum output power, the coupling efficiency from a VCSEL and the stability of radiation angles are discussed.

## 2 Structure

Figure 1 (a) shows the proposed structure of a tunable VCSEL laterally integrated with a semiconductor optical amplifier (SOA). Electrodes for carrier injection are formed on both VCSEL and SOA separately. The layer structure is almost the same as the MEMS VCSEL we demonstrated [11]. An active layer that consists of 980 nm multiple quantum wells, oxide layer and variable air gap are sandwiched by a pair of distributed Bragg reflector mirrors (DBR). The air gap is formed by selective chemical etching to a GaAs sacrificial layer. The top DBR is mechanically actuated, which leads to the change of a cavity length, i.e., the change of the lasing wavelength of the VCSEL. The Bragg reflector waveguide in the slow light SOA section can support slow light traveling modes thanks to its large waveguide dispersion [15]. Optical- and carrier-confinement is provided by an oxide layer which is formed by selective oxidation of an aluminum rich layer. The lateral oxide aperture width is assumed to be  $5\ \mu\text{m}$  for the single mode operation of the VCSEL. The vertical radiation from VCSEL cavity is suppressed by adding a metal mirror on the top DBR. The lateral optical coupling takes place between the VCSEL and the slow light SOA through a narrow oxidized region (a few micrometers wide). A slow light propagation is directly excited from a VCSEL. The output can be taken from a slow light amplifier by decreasing its top-DBR reflectivity to 98%. The radiation loss can be compensated by adding gain in an active region. If the gain of the active region is balanced with the total loss in the slow light waveguide, the radiated light intensity can be constant in the propagating direction. The total output power increases in proportion to the length of SOA if the entire beam is collected with an appropriate optics. It is noted that the carrier injection level into the SOA must be below threshold to prevent the lasing of SOA itself.

## 3 Modeling

We calculated the coupling efficiency between a VCSEL and a slow light SOA. The calculation model is shown in Fig. 1 (b). For simplicity, we use two-dimensional model. Optical field is calculated using a film-mode-

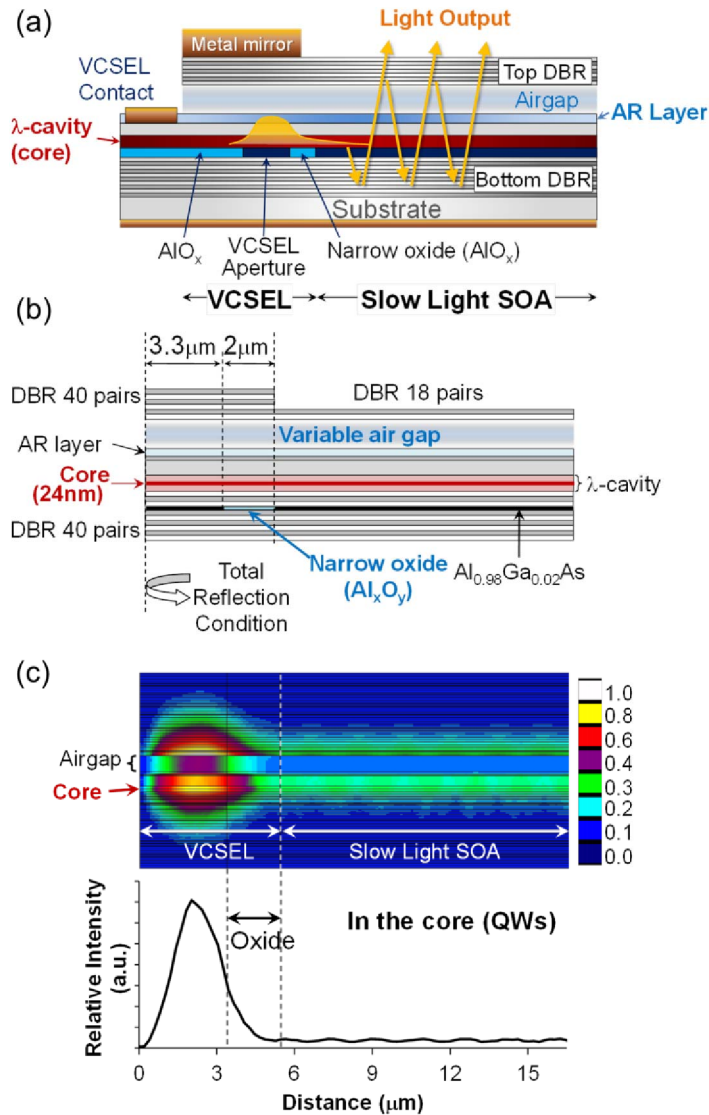


**Fig. 1.** (a) Schematic structure of our proposed device with integrated MEMS VCSEL and slow light SOA. A slow-light propagation mode of SOA is excited directly by the VCSEL, and optical output is taken from top DBR of the SOA. (b) Calculation model. (c) Calculated intensity distribution of optical field. Relative intensity profile in the core is shown in the bottom figure. No gain or absorption is considered in this calculation.

matching method (FIMMWAVE, Photon Design Co.) [16]. Both top- and bottom-DBRs are assumed 40 pair to suppress the vertical radiation. The layer structure is designed to have a cut-off wavelength of 982 nm, which is corresponding to the resonant wavelength for plane wave. The structure is the same as our MEMS VCSEL [12] except for the 3.5-pair DBR inserted between an active region and an oxidized layer to increase the lateral coupling efficiency. The active region is replaced by a 24 nm thick bulk GaAs active layer. The aperture size in the VCSEL section is assumed to be around 3 μm, and the oxide region in the left side is replaced by a total-reflection bound-

ary condition. A slow light mode of the Bragg reflector waveguide is excited from the left side of the model. A standing wave is formed by the almost 100% reflection from a narrow oxide region. Penetrated light couples to a slow-light propagation mode through a narrow oxide region. The width of a narrow oxide region between VCSEL and SOA is 2 μm which is optimized to have a high coupling efficiency. We define the coupling efficiency as

$$1/\tau_{\text{out}} = |E_0|^2 v_g / \int_{\text{VCSEL}} |E|^2 dz \quad (1)$$

$$\eta = \frac{1/\tau_{\text{out}}}{1/\tau_{\text{int}} + 1/\tau_{\text{out}}}, \quad (2)$$

where  $\int |E|^2 dz$  is the integral of the optical field intensity in the VCSEL cavity,  $E_0$  is the electric field amplitude at the boundary of VCSEL and SOA, and  $v_g$  is group velocity of the slow light. That is, Eq. (1) corresponds to the radiation loss per unit time from the VCSEL cavity. The dominator of Eq. (2) represents the total loss of the VCSEL. Namely, the coupling efficiency here is equivalent to the differential quantum efficiency defined in a conventional VCSEL. We assumed that the absorption loss in a VCSEL cavity is 20 cm<sup>-1</sup> and hence  $1/\tau_{\text{int}} = 5.8$  ps. It is confirmed that the scattering loss at the oxide boundary of a VCSEL and an SOA is negligibly small. Figure 1 (c) shows the calculated intensity distribution. A portion of the light confined in the VCSEL cavity penetrates into the SOA section through a narrow oxide and lateral coupling can be clearly seen.

Figure 2 (a) shows the calculated lasing wavelength of a tunable VCSEL with different air gaps and the calculated coupling efficiency in the tuning range. A coupling efficiency of over 40% can be seen for the entire wavelength tuning limited by free-spectral-range (FSR). The coupling efficiency becomes larger in longer wavelength since the effective refractive index step in the oxide region becomes smaller.

Next, we calculated the saturation characteristic of the integrated SOA to estimate the maximum output power using the following rate equations.

$$\frac{dN}{dt} = \frac{I}{eV} - BN^2 - CN^3 - f v_g g S \quad (3a)$$

$$\frac{dS}{dz} = (f\Gamma g - (\alpha_r + \alpha_i)) \cdot S \quad (3b)$$

$N$  is carrier density,  $S$  is photon density,  $V$  is the volume of active region,  $q$  is elementary charge,  $B$  and  $C$  are recombination coefficients,  $v_g$  is the group velocity of a slow light mode,  $g$  is a material gain coefficient per unit length in an active layer,  $\Gamma$  is an optical confinement factor and  $f$  is a slow down factor that is defined as the ratio of  $v_g$  to light velocity in bulk semiconductor material.  $\alpha_r$  and  $\alpha_i$  denote the radiation loss and the absorption loss per unit length for a slow light propagation mode, respectively. These losses are given from the decay rate of the calculated intensity distribution of a slow light mode. Thus, these losses include the effect of slowing light. The material absorption loss of the top and bottom DBRs are assumed as 10 cm<sup>-1</sup> and

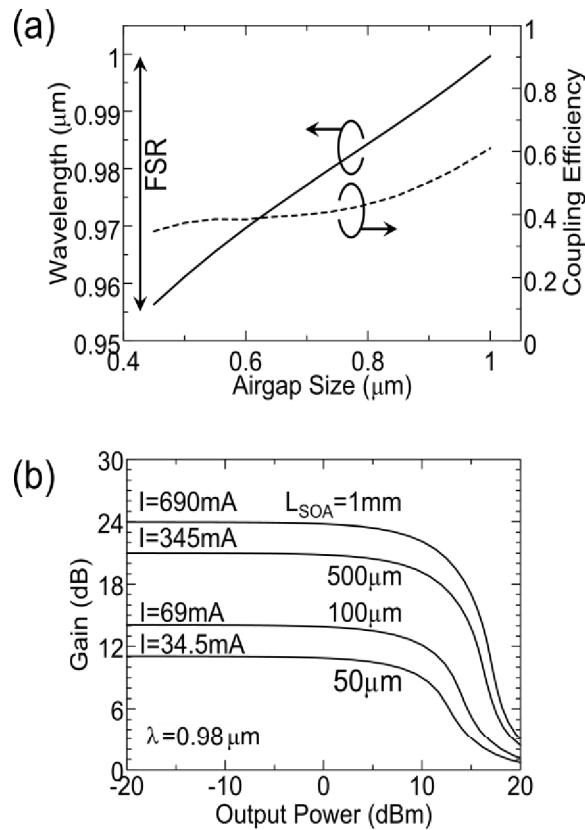


**Fig. 2.** (a) Calculated resonant wavelengths of VCSEL cavity and coupling efficiency as a functions of air gap size. (b) SOA gain as a function of output power for different SOA length.

$5 \text{ cm}^{-1}$ , respectively. The total output power radiated from the SOA section is given by

$$P_{out} = \int_0^L \frac{(S \cdot \alpha_r) w d v_g h \nu}{\Gamma} dz, \quad (4)$$

where  $w$ ,  $d$  and  $L$  represent the width, the thickness and the length of the active region of the SOA section, respectively. The SOA gain is defined as the ratio of coupling power into the SOA from the VCSEL and the total radiated power into free space in the following equation.

$$G = 10 \log(P_{out}/P_{in}). \quad (5)$$

We calculated the SOA gain by solving the rate equations (3a) and (3b) numerically. Figure 2(b) shows the calculated SOA gain as a function of output power for different SOA lengths. The number of pairs for the top DBR is assumed to be 16 pairs. The injection current density in the SOA section is determined to be  $13.8 \text{ kA/cm}^2$  for balancing the gain and the radiation loss. The corresponding injection current is shown for each SOA length. The saturation power of more than 10 mW with a small-signal gain of 11 dB is predicted for a  $50 \text{ μm}$ -long compact SOA. Larger output power can be taken with increasing the length of the SOA section. For example, a high output power of 16 dBm is expected when a VCSEL power of 1 mW is coupled to a 1 mm long SOA.

Finally, we calculated the electric field amplitude distribution in different wavelengths in order to visualize the output beam from the SOA in a linear gain regime as shown in Fig. 3. The injection current of a 50  $\mu\text{m}$  long SOA with an 18 pair top DBR is 4.6 mA for loss-compensation. A highly coherent beam is radiated from the SOA, and we can observe its clear constant phase fronts. In addition, it is noted that the radiation angle of 6.7 degrees is fixed during wide wavelength tuning operations. It is very different from our optical beam scanner based on a slow light optical amplifier exhibiting a large change of radiation angles associated with wavelength tuning [17]. While the output beam is highly elliptical, the output beam can be collected using optics incorporating an elliptical collimator thanks to its diffraction limited beam operation.

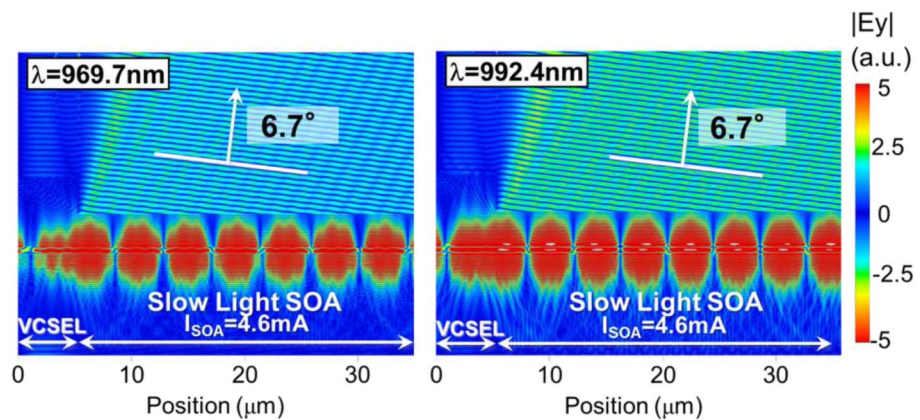


**Fig. 3.** Contour plots of electric field amplitude in different wavelengths in a linear gain regime. The SOA current with an 18 pair top DBR is 4.6 mA, which provides the gain that balances with total loss for 50  $\mu\text{m}$ -long SOA. It is clearly seen that a portion of the light, is radiated into free space and forms constant phase fronts. The radiation angle shows no noticeable change during wide wavelength tuning.

#### 4 Conclusion

We proposed the lateral integration structure of a MEMS tunable VCSEL and a slow light SOA to increase the single-mode power of a widely tunable VCSEL. The modeling predicts a high single-mode power of several tens mW with wavelength tuning range of over 40 nm. This novel integration scheme will enable high power and widely tunable on-chip light source with small-footprint. A drawback in MEMS tunable VCSELs that is a low single-mode power can be solved for use in optical communications and optical sensing.

#### Acknowledgments

This work was supported by Grant-in-Aid for Scientific Research (S) from

the Ministry of Education, Culture, Sports, Science and Technology of Japan  
(#22226008).